Supplemental material

Reda and Chandra, https://doi.org/10.1085/jgp.201711974

Supplemental materials and methods

Expression and purification of recombinant guinea pig cardiac troponin subunits

Recombinant *c-myc*–tagged guinea pig TnT (TnT_{WT} and TnT_{F88L}), guinea pig WT TnI, and guinea pig WT TnC were generated and cloned into a pSBETa vector (GenScript USA). The inclusion of the *c-myc* tag has been previously shown to have no effect on contractile function (Tardiff et al., 1998; Montgomery et al., 2001; Chandra et al., 2005). Recombinant DNA was transformed and expressed in BL21*DE3 cells (Invitrogen). The cells were cultured in terrific broth composed of the following: 1.2% tryptone (wt/vol), 2.4% yeast extract (wt/vol), 16.2 mM monobasic potassium phosphate, 53.9 mM dibasic potassium phosphate, and 0.4% glycerol (vol/vol). After overnight growth, the cells were spun down and sonicated in extraction buffer containing 50 mM Tris base, 6 M urea, 5 mM EDTA, pH 8.0, at 4°C, and a cocktail of protease inhibitors (5 mM benzamidine-HCl, 0.4 mM PMSF, 1 mM DTT, and 0.01% sodium azide [NaN_3]). The sonicated sample was spun down to separate the supernatant containing the desired protein. For TnT purification, the supernatant was subjected to ammonium sulfate fractionation (45% followed by 70%); the pellet was resuspended in 50 mM Tris base, 6 M urea, 1 mM EDTA, pH 8.0, at 4°C, 0.4 mM PMSF, 4 mM benzamidine-HCl, 1 mM DTT, and 0.01% NaN_3 and dialyzed against the same buffer overnight. The dialysate was loaded onto a DEAE-Fast Sepharose ion-exchange column (GE Healthcare Biosciences) and washed with buffer containing 50 mM Tris base, 6 M urea, 5 mM EDTA, pH 8.0, at 4°C, and a cocktail of protease inhibitors to further remove impurities. A salt gradient of 0–0.4 M NaCl was then applied to elute the samples containing the TnT protein (Mamidi et al., 2013). For TnI, the supernatant was loaded on CM Sepharose ion-exchange column (Healthcare Biosciences). A wash buffer containing 50 mM Tris base, 6 M urea, 1 mM EDTA, pH 8.0, at 4°C, and a cocktail of protease inhibitors was used to further remove impurities. A salt gradient of 0–0.3 M NaCl was then applied to elute the samples containing the TnI protein (Mamidi et al., 2013). For TnC purification, the supernatant was loaded on a DE-52 column, washed, and eluted with a salt gradient of 0–0.3 M NaCl. Samples containing TnC were pooled and dialyzed against a buffer containing 50 mM Tris base, 1 M NaCl, 5 mM $CaCl_2$, pH 7.5, at 4°C, and a cocktail of protease inhibitors. The dialysate was then loaded onto a phenyl Sepharose column and eluted with a buffer containing 50 mM Tris base, 1 M NaCl, 10 mM EDTA, pH 7.5, at 4°C, and a cocktail of protease inhibitors (Mamidi et al., 2013). All samples were assessed for purity on a 12.5% SDS gel. The desired samples were dialyzed extensively against 4 liters of deionized water containing 15 mM β-mercaptoethanol (0.25%), lyophilized, and stored at −80°C.

Preparation of detergent-skinned guinea pig cardiac muscle fibers

Guinea pigs were deeply anesthetized using isoflurane, and hearts were quickly excised and placed into an ice-cold high-relaxing solution containing the following: 20 mM BDM, 50 mM BES, pH 7.0, 30.83 mM potassium propionate (K-prop), 10 mM NaN_3, 20 mM EGTA, 6.29 mM $MgCl_2$, 6.09 mM Na_2ATP, 1.0 mM DTT, and a cocktail of protease inhibitors (4 mM benzamidine-HCl, 5 µM bestatin, 2 µM E-64, 10 µM leupeptin, 1 µM pepstatin, and 200 µM PMSF). Left ventricular papillary muscle bundles were carefully removed and dissected into smaller sections measuring 150–200 µm in thickness and 2–2.5 mm in length. Muscle fibers were then detergent skinned overnight by incubating at 4°C in high-relaxing solution containing 1% Triton X-100.

Western blot analysis

To quantify the level of incorporation of recombinant TnT (i.e., the amount of total endogenous TnT that was replaced by *c-myc*–tagged TnT_{WT} or TnT_{F88L}), Western blot analysis was performed. Reconstituted muscle fibers were solubilized in 2.5% SDS solution, and final concentrations were adjusted to 1 mg/ml by diluting in protein loading dye containing the following: 125 mM Tris-HCl, pH 6.8, 20% glycerol, 2% SDS, 0.01% bromophenol blue, and 50 mM β-mercaptoethanol. Equal amounts (10 µg) of protein samples were loaded and run on an 8% SDS gel to separate the endogenous and recombinant (*c-myc*–tagged) TnT according to their molecular weights. Proteins were then transferred to a polyvinylidene difluoridemembrane for Western blot analysis using a Trans-Blot Turbo transfer system (Bio-Rad Laboratories). TnT was probed using a monoclonal anti–TnT primary antibody (M401134; Fitzgerald Industries), followed by an HRP-labeled anti–mouse secondary antibody (RPN 2132; Amersham Biosciences). Densitometric analysis of protein profiles was performed to quantify the level of incorporation of recombinant TnT in reconstituted muscle fiber samples as follows. The optical band intensities of the endogenous TnT and recombinant TnT protein profiles were determined using ImageJ (National Institutes of Health). The total optical band intensity (the total amount of TnT expressed) was taken as the sum of the optical band intensities of endogenous and recombinant TnT protein. The incorporation level of recombinant TnT was determined by dividing the optical band intensity of the recombinant TnT protein profile by the total band intensity.

Composition of pCa solutions

The compositions of pCa solutions were calculated based on the program by Fabiato and Fabiato (1979). Two stocks of pCa solutions, pCa 4.3 and 9.0, were first made. pCa 4.3 solution contained the following: 50 mM BES, 5 mM NaN_3, 10 mM phosphoenol pyruvate,

10 mM EGTA, 10.11 mM $CaCl_2$, 6.61 mM $MgCl_2$, 5.95 mM Na_2ATP, and 31 mM K-prop. pCa 9.0 solution contained the following: 50 mM BES, 5 mM NaN_3, 10 mM phosphoenol pyruvate, 10 mM EGTA, 0.024 mM $CaCl_2$, 6.87 mM $MgCl_2$, 5.83 mM Na_2ATP, and 51.14 mM K-prop. All intermediate pCa solutions were made by mixing appropriate amounts of pCa 4.3 and 9.0 solutions (Fabiato and Fabiato, 1979). The pH and ionic strength of all pCa solutions were adjusted to 7.0 and 180 mM, respectively.

Measurement of muscle fiber mechanodynamics

Upon attainment of maximal steady-state activation, the motor arm was commanded to elicit various amplitude stretch/release perturbations (±0.5, ±1.0, ±1.5, and ±2.0% of the initial ML) to the attached muscle fibers (Ford et al., 2010). Each length perturbation was maintained for 5 s, and the corresponding force responses were recorded highlighting three different phases. As described previously (Ford et al., 2010), an NLRD model was fitted to the force response phases to estimate five model parameters: the magnitude of the instantaneous increase in force caused by a sudden increase in ML (E_D); the rate by which force drops because of dissipation of strain within bound XBs (c); a nonlinear interaction term representing the negative effect of strained XBs on other force-bearing XBs (γ); the rate by which XBs are recruited into the force-bearing state at the new ML (b); and the magnitude of increase in steady-state force caused by recruitment of additional force-bearing XBs at the increased ML (E_R). Fig. 1 depicts the length protocol of 2% sudden stretch (Fig. 1 A) and the corresponding force response (Fig. 1 B) from a muscle fiber. The physiological significance of each model parameter is explained below.

E_D: In phase 1, a sudden increase in ML (Fig. 1 A) causes an instantaneous increase in force from the isometric steady-state value (F_{ss}) to F_1 (Fig. 1 B). F_1 results from the distortion of the elastic elements within strongly bound XBs. Thus, F_1 increases when the number of strong XBs in the steady state, before ML change, is higher, and vice versa. E_D is estimated as the slope of the relationship between changes in F_1–F_{ss} and the imposed changes in ML (ΔL), and thus provides an approximate measure of the number of strongly bound XBs (Campbell et al., 2004; Ford et al., 2010).

c: In phase 2, as the muscle fiber is maintained at the increased ML (Fig. 1 A), force rapidly decays to a minimum point at a characteristic rate, c (Fig. 1 B). This rapid decay in force results from the detachment of XBs; c provides an approximate measure of XB detachment rate, g (Campbell et al., 2004).

γ: The parameter γ represents the negative impact of strained XBs on the recruitment of other force-bearing XBs, an effect that is mediated by allosteric/cooperative properties that exists within the thin filament. When the negative effect of strained XBs on the state of other force-bearing XBs is less pronounced, the magnitude of force decline is lesser; that is, the nadir is less pronounced and γ is attenuated. Thus, a decrease in γ suggests that TnT-induced changes in thin filament cooperativity attenuate the effect of strained XBs on other force-bearing XBs.

b: In phase 3, as the muscle is held at the increased ML (Fig. 1 A), force begins to rise gradually in an exponential fashion at a characteristic rate, b (Fig. 1 B). This gradual rise in force results from the recruitment of XBs into the force-bearing state corresponding to the increase in ML.

E_R: The rise in force during phase 3 levels off to a new steady-state value (F_{nss}) that is higher than F_{ss} (Fig. 1 B). The magnitude of increase, from F_{ss} to F_{nss}, is proportional to the number of additional force-bearing XBs recruited for the given increase in ML. Parameter E_R is derived as the slope of the relationship between changes in F_{nss}–F_{ss} and ΔL, and thus represents the magnitude of ML-mediated increase in XB recruitment.

Rate constant of tension redevelopment

k_{tr} was estimated using a modified version of the large slack/restretch maneuver originally designed by Brenner and Eisenberg (1986) and is described in our earlier published works (Ford et al., 2012; Gollapudi et al., 2012, 2013). During maximal Ca^{2+} activation (pCa 4.3), muscle fibers are rapidly slackened by 10% of the initial ML using a servo motor and maintained at the reduced length for 25 ms. Muscle fibers are then rapidly (0.5 ms) stretched past the initial ML by 10% and instantly returned to initial ML, where the muscle fiber starts to redevelop force as detached XBs equilibrate into force-bearing states. k_{tr} is estimated by fitting the following monoexponential function to the rising phase of the resulting force response:

$$F = (F_{ss} - F_{res})\left(1 - e^{-k_{tr}t}\right) + F_{res},$$

where F_{ss} is the steady-state isometric force and F_{res} is the residual force from which the fiber starts to redevelop force.

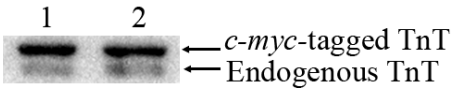

Figure S1. **Western blot of reconstituted muscle fibers.** A representative Western blot showing the level of recombinant TnT (*c-myc*–tagged TnT_{WT} or *c-myc*–tagged TnT_{F88L}) incorporation in muscle fibers reconstituted with TnT_{WT} or TnT_{F88L}. Reconstituted muscle fibers were solubilized in 2.5% SDS solution and separated on a standard 8% SDS gel. TnT was transferred from an 8% SDS gel to a polyvinylidene difluoride membrane and probed with a monoclonal anti-TnT primary antibody, followed by an HRP-labeled anti–mouse secondary antibody. Lane 1 represents muscle fibers reconstituted with *c-myc*–tagged TnT_{WT}, and lane 2 represents muscle fibers reconstituted with *c-myc*–tagged TnT_{F88L}. Densitometric analysis (ImageJ) revealed that the incorporation level of *c-myc*–tagged TnT_{WT} was 77 ± 6%, and that of *c-myc*–tagged TnT_{F88L} was 72 ± 7%. Values reported as mean ± SD; $n = 3$.

Table S1. **Effect of TnT_{F88L} on various dynamic contractile parameters at comparable levels of force production during submaximal activation**

Parameter	1.9 µm		2.3 µm	
	TnT_{WT}	TnT_{F88L}	TnT_{WT}	TnT_{F88L}
E_D (mN · mm^{-3})	449 ± 27	521 ± 41[a]	667 ± 41	677 ± 23[a]
c (s^{-1})	13.81 ± 0.25	12.92 ± 0.61[a]	9.81 ± 0.78	9.38 ± 0.26[a]
b (s^{-1})	3.55 ± 0.13	3.34 ± 0.15[a]	3.61 ± 0.23	3.32 ± 0.11[a]
γ (s^{-1})	40.08 ± 1.16	29.73 ± 2.13***	25.11 ± 2.9	24.05 ± 1.74[a]
E_R (mN · mm^{-3})	65.01 ± 6.58	112.1 ± 5.98**	212.7 ± 23.2	209.1 ± 12.4[a]
k_{tr} (s^{-1})	1.69 ± 0.06	1.52 ± 0.08[a]	1.50 ± 0.04	1.42 ± 0.06[a]

Dynamic contractile parameters at short SL were compared at pCa 5.3 (TnT_{WT}) and pCa 5.5 (TnT_{F88L}) because of similar levels of force production; 19.59 ± 0.91 mN/mm^2 for TnT_{WT} and 21.41 ± 1.54 mN/mm^2 for TnT_{F88L}. At long SL, dynamic contractile parameters were compared at pCa 5.4 (TnT_{WT}) and pCa 5.5 (TnT_{F88L}); tension was 33.13 ± 2.64 mN/mm^2 for TnT_{WT} and 34.09 ± 1.04 mN/mm^2 for TnT_{F88L}. Estimates from several muscle fibers per group were averaged and presented as mean ± SEM. Statistical differences were analyzed using two-way ANOVA and subsequent post hoc multiple pairwise comparisons (Fisher's LSD method). The number of fibers measured were as follows: 5 and 10 for TnT_{WT} at short and long SL, respectively; 10 and 9 for TnT_{F88L} at short and long SL, respectively. Asterisks indicate significant difference compared to TnT_{WT} fibers (**, $P < 0.01$; ***, $P < 0.001$).
[a]Not significant.

References

Brenner, B., and E. Eisenberg. 1986. Rate of force generation in muscle: correlation with actomyosin ATPase activity in solution. *Proc. Natl. Acad. Sci. USA.* 83:3542–3546. https://doi.org/10.1073/pnas.83.10.3542

Campbell, K.B., M. Chandra, R.D. Kirkpatrick, B.K. Slinker, and W.C. Hunter. 2004. Interpreting cardiac muscle force-length dynamics using a novel functional model. *Am. J. Physiol. Heart Circ. Physiol.* 286:H1535–H1545. https://doi.org/10.1152/ajpheart.01029.2003

Chandra, M., M.L. Tschirgi, and J.C. Tardiff. 2005. Increase in tension-dependent ATP consumption induced by cardiac troponin T mutation. *Am. J. Physiol. Heart Circ. Physiol.* 289:H2112–H2119. https://doi.org/10.1152/ajpheart.00571.2005

Fabiato, A., and F. Fabiato. 1979. Calculator programs for computing the composition of the solutions containing multiple metals and ligands used for experiments in skinned muscle cells. *J. Physiol. (Paris).* 75:463–505.

Ford, S.J., M. Chandra, R. Mamidi, W. Dong, and K.B. Campbell. 2010. Model representation of the nonlinear step response in cardiac muscle. *J. Gen. Physiol.* 136:159–177. https://doi.org/10.1085/jgp.201010467

Ford, S.J., R. Mamidi, J. Jimenez, J.C. Tardiff, and M. Chandra. 2012. Effects of R92 mutations in mouse cardiac troponin T are influenced by changes in myosin heavy chain isoform. *J. Mol. Cell. Cardiol.* 53:542–551. https://doi.org/10.1016/j.yjmcc.2012.07.018

Gollapudi, S.K., R. Mamidi, S.L. Mallampalli, and M. Chandra. 2012. The N-terminal extension of cardiac troponin T stabilizes the blocked state of cardiac thin filament. *Biophys. J.* 103:940–948. https://doi.org/10.1016/j.bpj.2012.07.035

Gollapudi, S.K., C.E. Gallon, and M. Chandra. 2013. The tropomyosin binding region of cardiac troponin T modulates crossbridge recruitment dynamics in rat cardiac muscle fibers. *J. Mol. Biol.* 425:1565–1581. https://doi.org/10.1016/j.jmb.2013.01.028

Mamidi, R., S.L. Mallampalli, D.F. Wieczorek, and M. Chandra. 2013. Identification of two new regions in the N-terminus of cardiac troponin T that have divergent effects on cardiac contractile function. *J. Physiol.* 591:1217–1234. https://doi.org/10.1113/jphysiol.2012.243394

Montgomery, D.E., J.C. Tardiff, and M. Chandra. 2001. Cardiac troponin T mutations: correlation between the type of mutation and the nature of myofilament dysfunction in transgenic mice. *J. Physiol.* 536:583–592.

Tardiff, J.C., S.M. Factor, B.D. Tompkins, T.E. Hewett, B.M. Palmer, R.L. Moore, S. Schwartz, J. Robbins, and L.A. Leinwand. 1998. A truncated cardiac troponin T molecule in transgenic mice suggests multiple cellular mechanisms for familial hypertrophic cardiomyopathy. *J. Clin. Invest.* 101:2800–2811. https://doi.org/10.1172/JCI2389